

P. Maget, H. Lütjens, B. Alper, M. Baruzzo, M. Brix, P. Buratti, R.J. Buttery,
C. Challis, R. Coelho, E. De la Luna, C. Giroud, N. Hawkes, G.T.A. Huysmans,
I. Jenkins, X. Litaudon, J. Mailloux, N. Mellet, D. Meshcheriakov,
M. Ottaviani and JET EFDA contributors

Non Linear MHD Modelling of NTMs in JET Advanced Scenarios

“This document is intended for publication in the open literature. It is made available on the understanding that it may not be further circulated and extracts or references may not be published prior to publication of the original when applicable, or without the consent of the Publications Officer, EFDA, Culham Science Centre, Abingdon, Oxon, OX14 3DB, UK.”

“Enquiries about Copyright and reproduction should be addressed to the Publications Officer, EFDA, Culham Science Centre, Abingdon, Oxon, OX14 3DB, UK.”

The contents of this preprint and all other JET EFDA Preprints and Conference Papers are available to view online free at www.iop.org/Jet. This site has full search facilities and e-mail alert options. The diagrams contained within the PDFs on this site are hyperlinked from the year 1996 onwards.

Non Linear MHD Modelling of NTMs in JET Advanced Scenarios

P. Maget¹, H. Lütjens², B. Alper³, M. Baruzzo⁴, M. Brix³, P. Buratti⁴, R.J. Buttery⁵,
C. Challis³, R. Coelho⁶, E. De la Luna⁷, C. Giroud³, N. Hawkes³, G.T.A. Huysmans¹,
I. Jenkins³, X. Litaudon¹, J. Mailloux³, N. Mellet¹, D. Meshcheriakov¹,
M. Ottaviani¹ and JET EFDA contributors *

JET-EFDA, Culham Science Centre, OX14 3DB, Abingdon, UK

¹*CEA, IRFM, F-13108 Saint Paul-lez-Durance, France*

²*Centre de Physique Théorique, Ecole Polytechnique, CNRS, France*

³*EURATOM-CCFE Fusion Association, Culham Science Centre, OX14 3DB, Abingdon, OXON, UK*

⁴*Associazione EURATOM-ENEA sulla Fusione, C.R. Frascati, Roma, Italy*

⁵*General Atomics, PO Box 85608, San Diego, CA 92186-5608, USA*

⁶*Institute Plasmas & Fusao Nucl, EURATOM Assoc, IST, P-1049001 Lisbon, Portugal*

⁷*Laboratorio Nacional de Fusión, Asociación EURATOM-CIEMAT, Madrid, Spain*

* See annex of F. Romanelli et al, "Overview of JET Results",
(23rd IAEA Fusion Energy Conference, Daejeon, Republic of Korea (2010)).

Preprint of Paper to be submitted for publication in Proceedings of the
23rd IAEA Fusion Energy Conference, Daejeon, Republic of Korea
(10th October 2010 - 16th October 2010)

ABSTRACT.

Advanced Tokamak Scenarios, with $q_{min} > 1$, often encounter MHD limits due to Kink or Resistive Wall Modes (RWM), or to Neoclassical Tearing Modes (NTM) that degrade performances or evolve to disruption. NTM on $q = 2$ is of particular concern in this respect, and we have investigated its non linear threshold on JET Advanced Scenarios using the non linear MHD code XTOR [1]. We show that in the experiment considered, the triggering of a (2,1) NTM is consistent with a critical island width that decays with time during the discharge, and results from a weakening of curvature stabilization as magnetic shear increases at the resonance. Plasma rotation, which has been evidenced as a stabilizing effect in several experimental devices, is also investigated. We show that plasma flow increases only moderately (about 5%) the critical island width in the experimental range. Conversely, in the low momentum torque limit (ITER), the threshold for (2,1) NTM excitation increases significantly (about 20%) with the magnetic Prandtl number $Pr_m = \mu_0 v / \eta$ between the perpendicular collisional ($Pr_m \sim 2$) and the toroidal turbulent ($Pr_m \sim 100$) values.

1. INTRODUCTION

Tokamak research towards long pulse operation (the so-called "Advanced Tokamak" scenario), addresses plasma discharges having a safety factor above unity ($q > 1$) and performances approaching ideal MHD limits. Neoclassical Tearing Modes (NTM), which are usually triggered by MHD activity at $q = 1$ in inductive scenarios, are however still limiting the reliability of Advanced Tokamak discharges, where they are triggered by other MHD modes (Edge Localized Modes, Fast particle driven modes, Resistive Wall Modes, ...). When triggered, the NTM growth leads to confinement degradation, and sometimes disruption. In this respect, the (2,1) NTM is of particular concern for ITER. The physics of NTM is characterized by its linear stability, due to the combined effect of pressure gradient and magnetic field curvature [2, 3, 4], and by a non linear drive provided by the bootstrap current perturbation [5], mediated by heat transport in the small island limit [6]. Several issues regarding NTM threat are investigated in present experiments, in particular the determination of the main operational parameters that influence NTM triggering. In recent years, attention has been paid to the role of current profile and plasma flow [7, 8, 9, 10]. In the present work, we study the stability properties and dynamics of the (2,1) NTM in a typical JET Advanced Tokamak discharge, using a non linear, full MHD code (XTOR [1]). We first show how the inductive current diffusion lowers the NTM threshold through the increase of the magnetic shear, and in a second part, we address the issue of NTM stabilization by plasma flow.

2. THRESHOLD FOR (2,1) NTM : ROLE OF MAGNETIC SHEAR

In the JET experiment that is considered, a (2,1) NTM is triggered after an ELM crash while the plasma performance is stationary but the magnetic equilibrium is still evolving. These conditions are ideal for investigating the role of the q -profile in the NTM threshold. This is obtained by inserting a finite seed at $q = 2$ into the system, and evolving the standard one fluid MHD model equations:

$$\begin{aligned} \partial_t p + \mathbf{V} \cdot \nabla p + \Gamma p - \mathbf{p} \cdot \nabla \mathbf{V} &= -\nabla \cdot \chi_{\perp} \frac{p}{\rho} + \nabla \cdot (\chi_{\parallel} - \chi_{\perp}) \frac{p}{\rho} + H \\ \partial_t \mathbf{B} &= \nabla \times (\mathbf{V} \times \mathbf{B}) - \nabla \times \eta (\mathbf{J} - \mathbf{J}_{\text{NI}}) \end{aligned} \quad (1)$$

$$\rho(\partial_t \mathbf{V} + \mathbf{V} \cdot \nabla \mathbf{V}) = \mathbf{J} \times \mathbf{B} - \nabla p + \nu \nabla^2 \mathbf{V}$$

where $\mathbf{J}_{\text{NI}} = \mathbf{J}_{\text{cd}} + \mathbf{J}_{\text{bs}}$ is the non inductive current density, \mathbf{J}_{bs} is the bootstrap current, \mathbf{J}_{cd} is the imposed current source ($\mathbf{J}_{\text{cd}} = (\mathbf{J} - \mathbf{J}_{\text{bs}})_{t=0}$), and $H = \nabla \cdot \chi_{\perp} \nabla p(t=0)$ is the heat source term. The bootstrap current is modelled as $\mathbf{J}_{\text{bs}} = \mathbf{J}_{\text{bs}}^{\text{eq}}(\nabla p(t)/\nabla p_{\text{eq}})B/B$. The magnetic equilibrium itself is computed with the CHEASE code [11], which also provides the equilibrium bootstrap current. The system is evolved using the fully implicit, non linear MHD code XTOR [1], starting from a toroidal equilibrium reconstruction constrained by Motional Stark Effect (MSE), polarimetry and core pressure measurements.

The critical island width (W_{crit}) is determined by increasing the size of the seed in XTOR until a non linear growth is obtained ($n = 0.1$ are evolved). As shown in figure 2 (top), the critical island width is decaying between $t = 6\text{s}$ and $t = 7\text{s}$ (the NTM is triggered at $t = 7.06\text{s}$), during the current diffusion, thus explaining that for a given level of MHD activity the (2,1) NTM is more easily excited at $t = 7\text{s}$. In order to better understand why the threshold decays with time, we formulate the problem in the extended Rutherford equation framework:

$$0.82S^{-1} \frac{dW}{dt} = a \Delta'(W) - 6.35 \frac{D_R}{\sqrt{W^2 + 0.65W_{\chi}^2}} + 6.35J_{\text{bs}} \frac{q}{s} \frac{D_R}{W^2 + (1.8W_{\chi})^2} \quad (2)$$

where the various terms are evaluated at $q = 2$, S is the Lundquist number ($S = \tau_R/\tau_A$, with $\tau_R = \mu_0 a^2/\eta$ and $\tau_A = R_0 \sqrt{\mu_0 \rho/B_0}$), $\bar{J}_{\text{bs}} \equiv (\mu_0 R_0/B_0)J_{\text{bs}}^{\text{eq}}$ with R_0 and B_0 the major radius and magnetic field at geometric axis, a the minor radius and $W \equiv w/a$ with w the island full width. We also note $W_{\chi} = 2\sqrt{2} (\chi_{\perp}/\chi_{\parallel})^{1/4} / \sqrt{x \epsilon} \text{ns}$, with $x = \sqrt{\Phi}$, Φ is the normalized toroidal flux, $s = d(\log q)/d(\log x)$ the magnetic shear and $\epsilon = a/R_0$. The resistive index D_R is defined in [2]. Considering the main dependencies in x and s of the simplified problem, i.e. $D_R \propto -xp'/s^2$, $W_{\chi} \propto 1/\sqrt{xs}$, $J_{\text{bs}} \propto -p'/\sqrt{x}$, and assuming a typical pressure profile $p = p_0(1 - x^2)^2$, we can calculate the (2,1) NTM threshold as a function of x and s from the above Extended Rutherford equation (assuming $a\Delta'(W) = 0$). During the diffusion of the plasma current, the position of the resonance increases only moderately, while the magnetic shear increases by more than 20% (figure 2). This evolution strongly reduces the amplitude of the curvature term ($D_R/W_{\chi} \propto 1/s^3$ with D_R varying from 0.47 to 0.27), and results in the decrease of the critical island width.

The reliability of the analytical prediction by the extended Rutherford model is actually strongly dependent on the importance of the curvature term. Indeed, this term balances the bootstrap drive in the absence of a significant Δ' contribution. When it becomes too small (because s is large for example), the Δ' term can be dominant, and usual simple estimates for this term do not provide a satisfactory evaluation of the critical island width [12].

The dynamics of the metastable (2,1) island and its impact on the energy confinement have been studied in non linear simulations where toroidal mode numbers from 0 to 6 are considered. In the simulations, magnetic diffusivity ($D_\eta \equiv \eta/\mu_0$) is larger than in the experiment, and heat diffusivity and viscosity need to be rescaled so that characteristic dimensionless numbers are conserved (Prandtl number $Pr \equiv \nu/\chi_\perp$ and magnetic Prandtl number $Pr_m \equiv \nu/D_\eta$, leading to a conservation of $\tau_R/\tau_E \sim \chi_\perp/D_\eta = Pr_m Pr$). Comparison with experimental dynamics requires accordingly a rescaling of the time scale

$$t_{(s)} = (D_\eta^{sim}/D_\eta^{exp}) T_A \bar{t}$$

where \bar{t} is the simulation time normalized to the Alfvén time. We can then superimpose the non linear simulation to the experimental measurements (figure 2), and a fair agreement is found for the characteristic time scale and amplitude of the confinement degradation.

3. INFLUENCE OF PLASMA ROTATION ON THE (2,1) NTM THRESHOLD

Several experiments have shown that plasma flow and its radial shear influences magnetic island saturation levels and stability [7, 8, 9, 10]. In particular, it was found that the performance threshold (N) at which an NTM is triggered decays with plasma rotation at the resonance. The theoretical understanding of the effect of flow shear on tearing modes does not provide unambiguous answers to experimentalists. Early works based on reduced MHD models predicted a destabilizing effect of flow shear on resistive instabilities in the sub-Alfvénic range [13, 14], while more recent models including parallel perturbations predict an effect that varies from destabilizing to stabilizing as viscosity increases [15], or a stabilizing effect in toroidal geometry without viscosity [16]. The use of a full MHD model, in the relevant toroidal geometry, including anisotropic heat transport and bootstrap current, allows us to clarify this issue.

The effect of bulk plasma rotation on NTM is addressed in the same model as before, but with a modified momentum equation:

$$\rho(\partial_t \mathbf{V} + \mathbf{V} \cdot \nabla \mathbf{V}) = \mathbf{J} \times \mathbf{B} - \nabla p + \nu \nabla^2 \mathbf{V} + \mathbf{M}$$

with a momentum source $\mathbf{M} = -\nu \nabla^2 \mathbf{V}_{src}$, and \mathbf{V}_{src} a prescribed toroidal flow velocity source. We choose two different rotation profiles covering the experimental range of velocity shear (defined as $a/L_\omega \equiv a d(\omega/\omega_A)/dR$, with $\omega = V_\varphi/R$ and $\omega_A = V_A/R_0 = 1/\tau_A$) (fig.3 and 4). If reported in the diagram of (2,1) NTM N threshold shown in the fig.7 of Ref.[7], the experimental velocity shear at $q = 2$ corresponds to a situation where the critical β_N should be about 40% higher than in the non rotating case.

The seed island is inserted after the plasma flow has reached equilibrium. As the seed is introduced, the plasma emits waves at characteristic frequencies: Alfvén waves (only observed in a low viscosity case and damped on $3-100\tau_A$), sound waves (damped in about $1000\tau_A$), and another oscillation whose frequency is related to the amplitude of the flow shear (rather than the flow) and that needs

more than 10000A to be damped (fig. 5 and 6).

The NTM threshold has been investigated in different viscosity conditions. Low viscosity conditions ($\text{Prm} = 2$) correspond to the perpendicular viscous force, where viscosity is expected to be due to collisions

$$v_{\perp, coll.} \approx 0.3 \frac{T_i v_i}{m_i \omega_{ci}^2}$$

with v_i the ion collision frequency and ω_{ci} the ion cyclotron frequency. High viscosity conditions ($\text{Prm} = 100$) correspond to the toroidal viscous force, expected to be dominated by the effect of turbulent transport. The toroidal Prm is calculated in TRANSP from the momentum balance (fig.7).

Results of simulations with $n=0, 1$ are shown in figure 8, where the critical island width for (2,1) NTM destabilization is plotted against the toroidal flow shear (left) and the toroidal flow (right) at $q = 2$. At a given Prm , the impact of flow on W_{crit} is found to be weak (about 5% increase within the experimental range of flow shear) for the two velocity profiles. Also, it seems that a better agreement is found when expressing W_{crit} as a function of flow rather than its shear.

In contrast with the weak effect of rotation, the critical island width increases significantly as Prm is increased. This could have a positive impact on the NTM threshold in ITER, where Prm might be larger due to lower resistivity.

These simulations do not recover expectations from experimental analysis. The intrinsic NTM stabilization that could be fitted (for saturated islands) by a reduction of Δ' with flow shear, and could qualitatively explain the increase of the β_N threshold [7, 9, 10], is clearly absent in the present results. Assuming that this effect is generic for tearing modes (and therefore independent on the details of the equilibrium, from Advanced Tokamak or Hybrid scenario discharges), we envisage four possible explanations for this disagreement. First, the parameter domain could play an important role, and we use a higher resistivity, although conserving other dimensionless quantities. Second, island deformation could be a key parameter, and we use so far only one toroidal mode number for the perturbation. Third, the MHD model could miss important physics: although a two fluid model may not be the key option because the polarization effect hypothesis does not seem to match the observations [7], it is possible that the large potential anisotropy of the viscous tensor (two orders of magnitude) affects the result. It is not excluded that the small perpendicular viscosity plays a more important role at low rotation and that the large toroidal viscosity matters as rotation becomes more important, thus yielding an overall stabilizing effect of plasma rotation on NTM stability. The last hypothesis, which is however not favoured by experimental analyses [7], is that the rotation effect comes from the impact of the flow on the primary mode and its coupling to the NTM. This first step in NTM triggering is independent from the NTM intrinsic stability.

In the future, we will investigate the first three options, the parameter domain, the non linear mode interaction, and viscous tensor anisotropy. One of these developments may clarify what is behind the favourable effect of flow on NTM threshold, thus allowing for an extrapolation to ITER.

SUMMARY

We have presented numerical investigations on (2,1) NTM threshold in a JET Advanced Tokamak discharge using a non linear full MHD code in toroidal geometry. This study covers issues like the current profile effect and the rotation effect in this magnetic configuration.

The main results can be summarized as follows:

- inductive current diffusion tend to lower NTM threshold through a weakening of curvature effect as magnetic shear increases at the resonance;
- the amplitude and dynamics of the confinement degradation is consistent between the simulation and the experiment (after proper rescaling of the time scale);
- toroidal rotation tends to increase the NTM threshold, but this effect is weak for a given Prm (about 5% in the range of experimental investigations), and this tendency holds for both low and high Prm ;
- in the low momentum input situation of ITER, a high value of the magnetic Prandtl number (which could result from a lower resistivity) is favourable (larger critical width for NTM excitation);
- the hypothesis of a reduction of θ by flow shear, based on experimental results for NTM saturation, is not recovered by simulations;
- three options are being investigated for explaining this disagreement: the role of resistivity, the non linear mode interaction, and the effect of viscous tensor anisotropy.

ACKNOWLEDGMENTS

This work was carried out within the framework the European Fusion Development Agreement (EFDA) and the French Research Federation for Fusion Studies (FR-FCM). It was performed using HPC resources from GENCI-IDRIS (Grant 2010-056348). It is supported by the European Communities under the contract of Association between Euratom and CEA. The views and opinions expressed herein do not necessarily reflect those of the European Commission.

REFERENCES

- [1]. Lütjens H. et al., Journal of Computational Physics **229** (2010) 8130 .
- [2]. Glasser A.H. et al., Physics of Fluids **18** (1975) 875.
- [3]. Kotschenreuther M. et al., Physics of Fluids **28** (1985) 294.
- [4]. Lütjens H. et al., Physics of Plasmas **8** (2001) 4267.
- [5]. Carrera R. et al., Physics of Fluids **29** (1986) 899.
- [6]. Fitzpatrick R. Physics of Plasmas **2** (1995) 825.
- [7]. Buttery R.J. et al., Physics of Plasmas **15** (2008) 056115.
- [8]. Gerhardtts S. et al., Nuclear Fusion **49** (2009) 032003.
- [9]. Hayre R.J.L. et al., Physics of Plasmas **16** (2009) 022107.
- [10]. Hayer R.J.L. et al., Physics of Plasmas **17** (2010) 056110.
- [11]. Lütjens H. et al., Computer Physics Communications **97** (1996) 219.

- [12]. Maget P. et al., Nuclear Fusion **50** (2010) 045004.
 [13]. EINAUDI G. et al., Physics of Fluids **29** (1986) 2563.
 [14]. Chen X.L. et al., Physics of Fluids B **2** (1990) 495.
 [15]. Coelho R. et al., Physics of Plasmas **14** (2007) 012101.
 [16]. Chandra D. et al., Nuclear Fusion **45** (2005) 524.

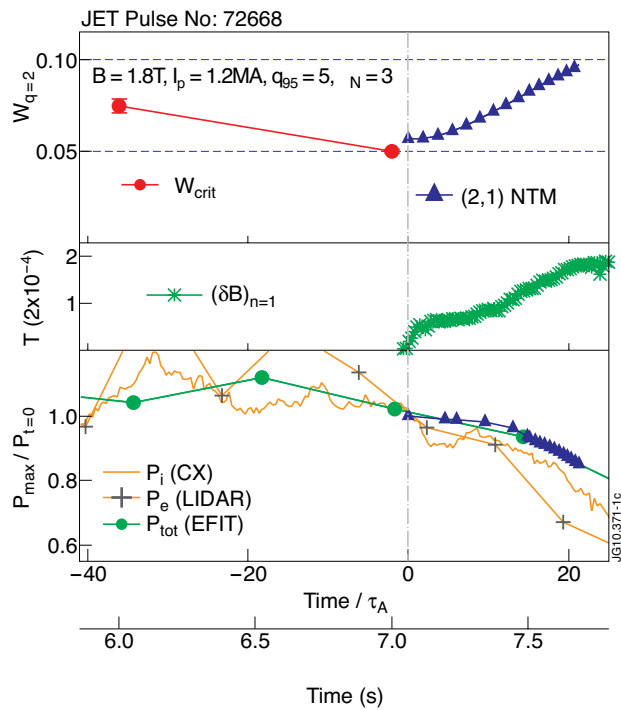


Figure 1: (2,1) NTM threshold (\bullet) and (2,1) island width (\blacktriangle) from XTOR (top); measured magnetic fluctuation amplitude (middle); dynamics of core pressure from diagnostics and from simulation (\blacktriangle).

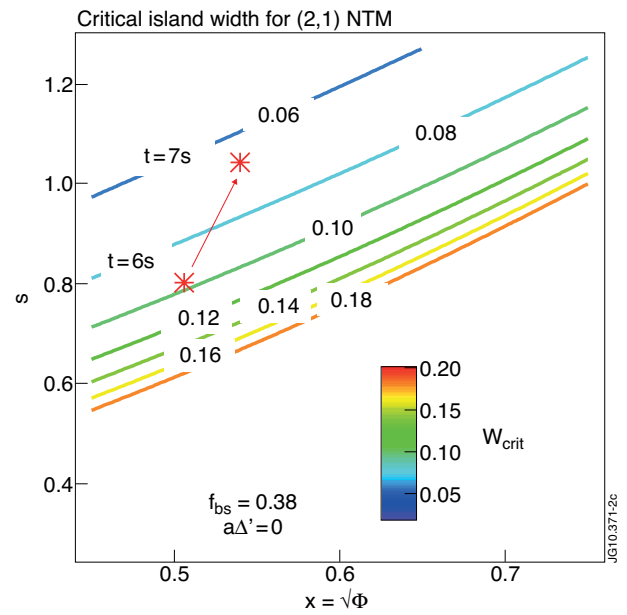


Figure 2: Contours of (2,1) NTM threshold as a function of radial coordinate of $q = 2$ and of magnetic shear, from Rutherford equation with $\Delta' = 0$.

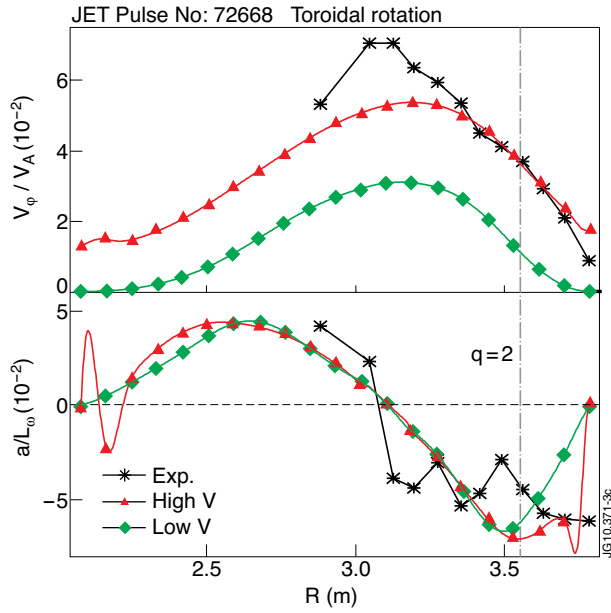


Figure 3: Velocity profiles from experiment and for simulations (top), and corresponding flow shear (bottom).

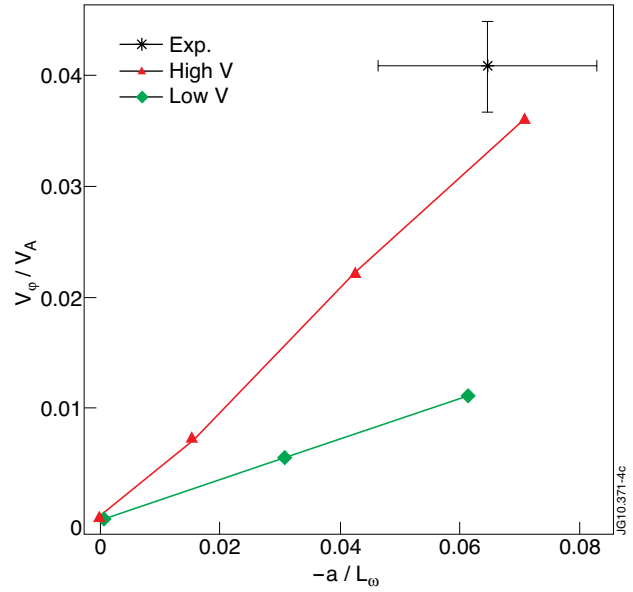


Figure 4: Velocity as a function of flow shear at the resonance for the two rotation sources.

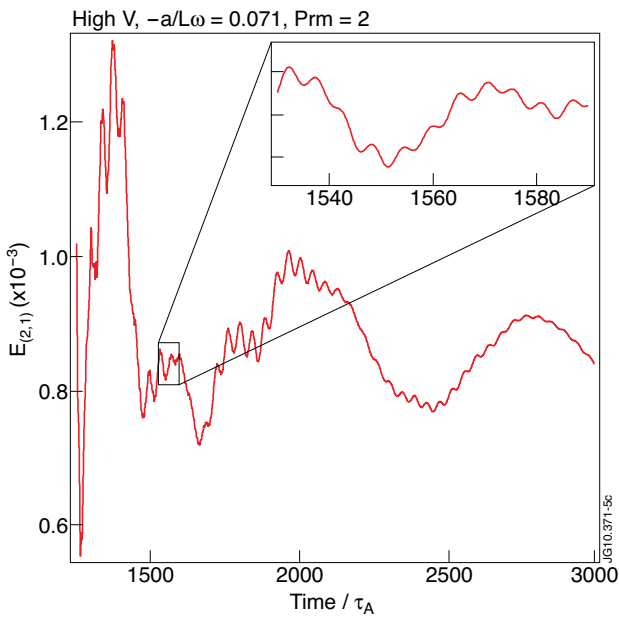


Figure 5: Wave emission induced by the seed (from (2,1) magnetic energy).

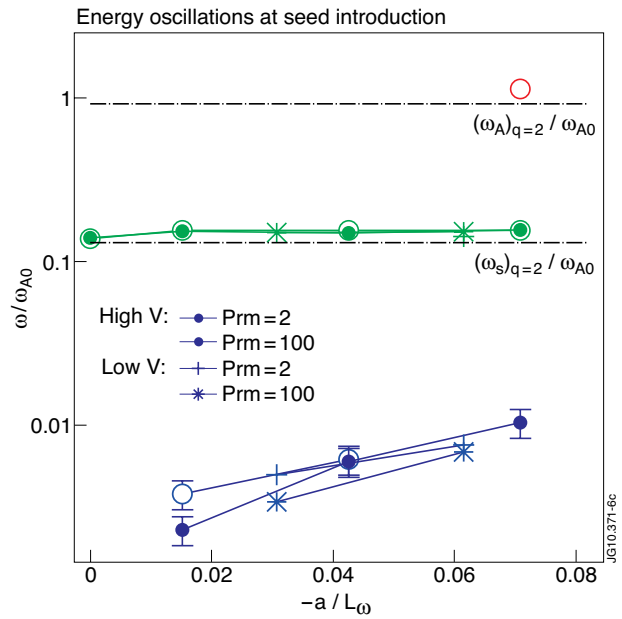


Figure 6: Frequency of the waves emitted at the introduction of the seed island, as a function of velocity shear.

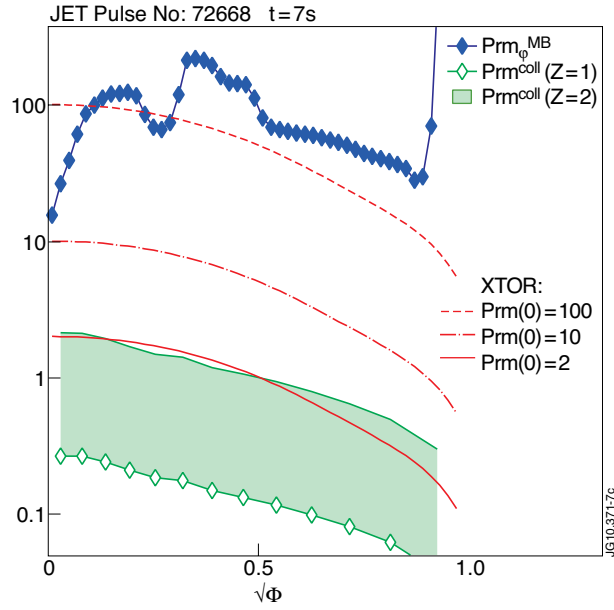


Figure 7: Magnetic Prandtl numbers from collisional viscosity and from toroidal momentum balance in TRANSP.

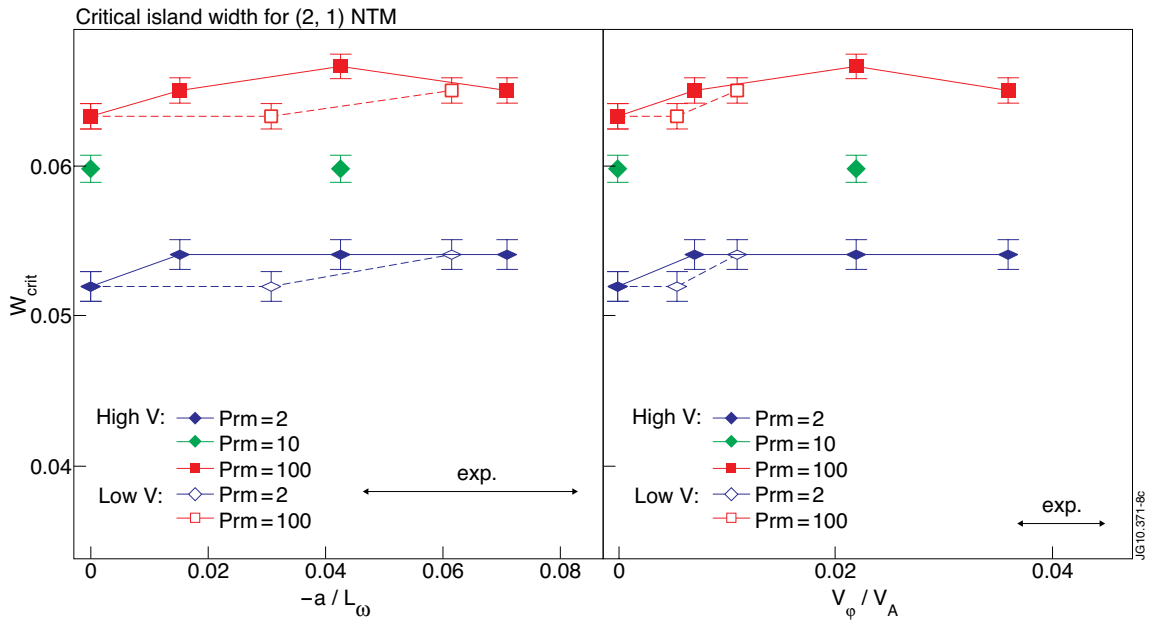


Figure 8: Critical island width as a function of flow shear (left) and flow (right) at $q = 2$ for the two velocity profiles and different viscosities.